

Selection of $Gd_2(WO_4)_3:Tb^{3+}$ for improving color deviation in white light-emitting diodes

Dieu An Nguyen Thi¹, Nguyen Doan Quoc Anh², Phan Xuan Le³

¹Faculty of Electrical Engineering Technology, Industrial University of Ho Chi Minh City, Ho Chi Minh City, Vietnam

²Faculty of Electrical and Electronics Engineering, Ton Duc Thang University, Ho Chi Minh City, Vietnam

³Faculty of Mechanical-Electrical and Computer Engineering, School of Engineering and Technology, Van Lang University, Ho Chi Minh City, Vietnam

Article Info

Article history:

Received Nov 30, 2021

Revised Jun 4, 2022

Accepted Jun 18, 2022

Keywords:

Color homogeneity

$Gd_2(WO_4)_3:Tb^{3+}$

Luminous flux

Monte Carlo theory

White-light-emitting diodes

ABSTRACT

This study successfully using the hydrothermal technique to synthesize $Gd_2(WO_4)_3:Tb^{3+}$ phosphors when subjected to calcination under the temperature of 900°C. Here are some aspects that were thoroughly examined: the crystal formation, photoluminescence, photoluminescence excitation, as well as fluorescent degradation for the samples. The $(Gd_{2-x}Tb_x)(WO_4)_3$ ($x=0.01-0.15$) phosphors exhibit a bright discharge of green under 547 nm ($^5D_4 \rightarrow ^7F_5$ shift for Tb^{3+}) when excited at 270 nm ($^4f_8 \rightarrow ^4f_7^5d_1$ shift for Tb^{3+}). Because of the exchange interaction between Tb^{3+} , the quenching concentration was determined to be around 10%. The addition of Tb^{3+} had no effect on the $(Gd_{2-x}Tb_x)(WO_4)_3$ phosphors' CIE chromaticity coordinates ($\sim 0.33 \pm 0.02$, $\sim 0.60 \pm 0.02$) or color temperatures (~ 5542 K). Nevertheless, when the Tb^{3+} content increased, the fluorescence lifespan for 547 nm emission reduced due to energy transfer between Tb^{3+} . The strong green emission from $Gd_2(WO_4)_3:Tb^{3+}$ phosphors is a potential element for white-light-emitting diodes (WLEDs) and display areas.

This is an open access article under the [CC BY-SA](https://creativecommons.org/licenses/by-sa/4.0/) license.



Corresponding Author:

Phan Xuan Le

Faculty of Mechanical-Electrical and Computer Engineering, School of Engineering and Technology

Van Lang University

Ho Chi Minh City, Vietnam

Email: le.px@vlu.edu.vn

1. INTRODUCTION

In recent decades, the development of innovative illumination apparatuses (including displaying screens, biosensors, and solid-state lasers) has widely use rare earth (RE^{3+}) doped glass, ceramics, and phosphors [1]-[3]. Because of the 4f electron layer arrangement of rare earth elements, the related compounds have a wide range of fluorescence properties. Because Tb^{3+} has a $4f^8$ power state as well as being easily influenced by its surroundings, samples containing Tb^{3+} have a superior fluorescent excitation as well as discharge spectrum [4]. Tb^{3+} also possesses an excited lengthy state duration as well as an uncomplicated discharge apex cleaving mode. As a result, fluorescent green materials research has focused on it [5]. However, $(WO_4)_3^{2-}$ and Gd^{3+} can sensitize the active ion, strengthening the active ion to excited green light within the $Gd_2(WO_4)_3$ matrix. As a result, the Tb^{3+} doping $Gd_2(WO_4)_3$ is critical in the research. We used a hydrothermal approach to synthesize Tb^{3+} doped $Gd_2(WO_4)_3$ phosphor, and we thoroughly investigated its luminous properties using X-ray diffraction (XRD), photoluminescence, photoluminescence excitation, as well as different techniques of assessment. Our team also investigated the production of the substance, stage layout, as well as fluorescent result.

2. EXPERIMENTAL DETAILS

Without additional purification, all the required chemical reagents are Gd_2O_3 and Tb_4O_7 (99.99%, Huizhou Ruier Rare Chemical Hi-Tech Co. Ltd., Huizhou, China); $Na_2WO_4 \cdot 2H_2O$ (99.5%), $NaOH$, (96%) and HNO_3 (AR) from Sinopharm Chemical Reagent Co. Ltd., Shanghai, China [6]. To begin the process, we dissolve Gd_2O_3 and Tb_4O_7 in hot nitric acid first. In the meantime, we also processed the obliged amount of $RE(NO_3)_3$ ($RE=Gd$ and Tb) solutions. According to the chemical formula of $(Gd_{2-x}Tb_x)(WO_4)_3$, our team obtained the mixture of salt alongside $RE(NO_3)_3$ as well as $Na_2WO_4 \cdot 2H_2O$. After finishing the above procedure, we dissolved a specific proportion of white $Na_2WO_4 \cdot 2H_2O$ particles in 50 ml water. Applying the same technique with a determined nitrate mixture portion combined with H_2O (20 ml), then stirring for about 5 minutes using one collector-type constant temperature magnetic stirring device. After the unrefined substances became perfectly mixed and dissolved into nitrate mixture, we poured it in the sodium tungstate mixture. The titration ceased after 30 minutes. Afterwards, we put $NaOH$ into the product then control the pH to 7. Then, transfer the reaction solution to a 100 ml stainless steel autoclave. Next, we placed the reaction kettle inside the oven setting to $120^\circ C$ with a 24-hour reaction period. In terms of eliminating the hydrothermal products, we cool the reaction kettle to standard temperature once the reaction is complete. The resulting hydrothermal substances was cleansed several times with deionized H_2O . Afterwards, we also cleansed them one more time with anhydrous ethanol by immersing them in ethanol ($80^\circ C$, let dry for 6 hours). We dried the precursor then calcined it in air under $900^\circ C$ for 2 hours to get the desired phosphor [7]-[9].

3. RESULTS AND ANALYSIS

The reversal shift in the concentrations of $Gd_2(WO_4)_3:Tb^{3+}$ as well as the phosphorus $YAG:Ce^{3+}$ are exhibited via Figure 1. The shown adjustment has an impact on the hue output as well as lumen performance of the WLED device, which involves keeping average CCT values and affecting the absorptivity as well as dispersion of the WLED device with a pair of phosphor sheets. The hue output value in the device depends on the $Gd_2(WO_4)_3:Tb^{3+}$ concentration that was chosen. When the $Gd_2(WO_4)_3:Tb^{3+}$ ratio increased from 2% to 20% Wt., the $YAG:Ce^{3+}$ content suffered a penalty so that the median CCT values can be maintained. Such a mechanic would also be true in the case of devices under between 5,600 K and 8,500 K.

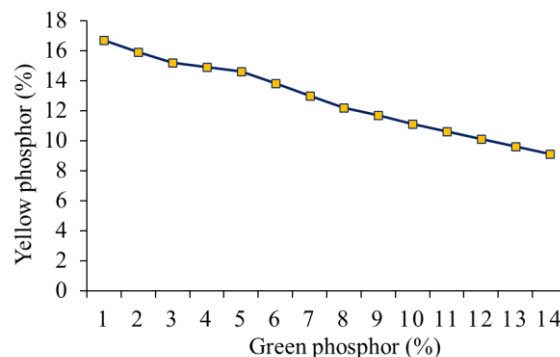


Figure 1. Sustaining median CCT values by altering phosphor content

The following formulas [10], [11] can be used to calculate the equivalent color temperature:

$$T = -437n^3 + 3601n^2 - 6861n + 5514.31 \quad (1)$$

and,

$$n = (x - 0.332)/(y - 0.1858) \quad (2)$$

for (~ 0.33 , ~ 0.60), the color temperature of the $(Gd_{1.90}Tb_{0.10})(WO_4)_3$ sample was determined to be nearly 5,542 K. Meanwhile, a recent study claimed all $(Gd_{2-x}Tb_x)(WO_4)_3$ phosphors possess the same CIE hue coordinate as well as hue temperature identified as $(0.33 \pm 0.02, 0.60 \pm 0.02)$ as well as 5,542 K.

Figure 2 depicts precisely the influence of the green phosphorus $Gd_2(WO_4)_3:Tb^{3+}$ concentration imposed on the transmitting spectrum in the WLED device. The production demands will decide what option to be chosen. WLED devices with good color fidelity will somewhat diminish luminous flux. As shown in Figure 2, white light is the spectral region's synthesis. These five figures show 4,000 K spectra. Obviously, the intensity surges as the $Gd_2(WO_4)_3:Tb^{3+}$ content goes up in two sections of the light spectrum: 420 nm-480 nm along with 500-640 nm. Higher final luminous flux may be seen in the two-band emission spectrum. Besides, the dispersion within the phosphorous layer as well as the device will increase as well, result in favored color uniformity. This eventuality is a significant outcome only when using $Gd_2(WO_4)_3:Tb^{3+}$. The color consistency in the remote phosphor layout under significant temperature, in particular, might be challenging to control. Our study found that $Gd_2(WO_4)_3:Tb^{3+}$, under color temperatures of 5,600 K as well as 8,500 K, can lead to the WLED device having greater hue output.

In the paper, we have further illustrated the emitted light flux performance for the remote phosphor layout with two sheets. The results in Figure 3 show that when the concentration of $Gd_2(WO_4)_3:Tb^{3+}$ increases (2%-20% wt.), the lumen emitted also increases dramatically. In all three average correlated color temperatures (CCTs), the color divergence was remarkably reduced with the phosphor $Gd_2(WO_4)_3:Tb^{3+}$ concentration, as shown in Figure 4. This event occurred because of the red phosphor layer's absorption. When $Gd_2(WO_4)_3:Tb^{3+}$ phosphor consumed the illumination in blue created from the chip in light-emitting diodes (LED), it metamorphoses the blue illumination, turning it green. Besides blue illumination, $Gd_2(WO_4)_3:Tb^{3+}$ particles also swallowed yellow illumination created by the said chip. However, the blue light absorption is mightier due to the material's absorption qualities. As a result of the addition of $Gd_2(WO_4)_3:Tb^{3+}$, the green illumination content inside the WLED device will surge, improving the color consistency index. Hue consistency would be among the very crucial factors in current WLEDs. The higher the hue consistency index, the greater the WLED's price. Though, the low cost for $Gd_2(WO_4)_3:Tb^{3+}$ is an advantage for applying in a variety of applications.

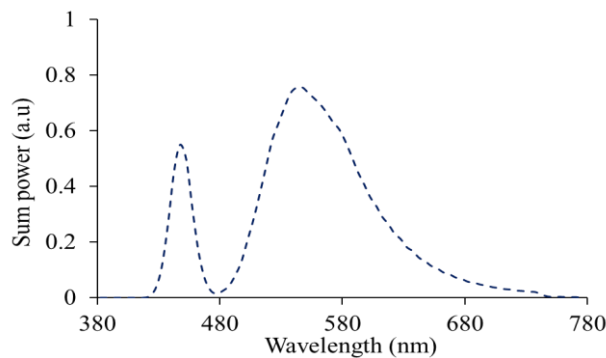


Figure 2. The relation between the discharge spectra in the 4,000 K WLED device and concentration

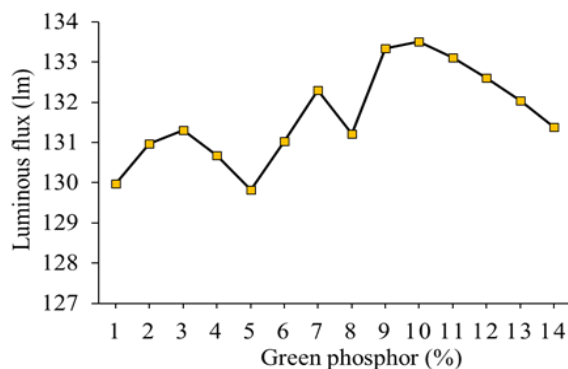


Figure 3. The luminous flux of WLEDs as a function of $Gd_2(WO_4)_3:Tb^{3+}$ concentration

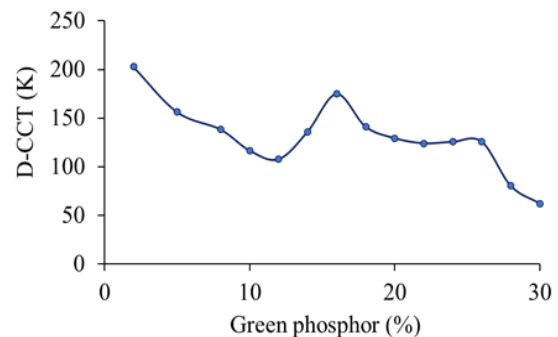


Figure 4. The color deviation of WLEDs as a function of $Gd_2(WO_4)_3:Tb^{3+}$ concentration

Calculating the constant s using the following formula yields the interactivity form for luminescent abatement of $\text{Gd}_2(\text{WO}_4)_3:\text{Tb}^{3+}$ [12]-[14]:

$$\log(I/c) = (-s/d)\log c + \log f \quad (3)$$

c represents the content of the trigger. I represents the strength of discharge. f represents a constant. s represents the electric multipole index. d represents the magnitude of the sample (with $d=3$ in the case of a conventional sample). The dipole-quadrupole, dipole-dipole, as well as quadrupole-quadrupole interactivities are represented by the s values 6, 8, and 10 correspondingly. Furthermore, $s=3$ denotes an exchange interaction. Figure 4 shows the relative connection among $\log(I/c)$ as well as $\log(c)$ under 547 nm discharge. We calculated the tilt ($-s/3$) to be -0.81 , resulting in s equal to roughly 2.43 for the $\text{Gd}_2(\text{WO}_4)_3:\text{Tb}^{3+}$ samples, showing that the energy transfer between $\text{Tb}^{3+}-\text{Tb}^{3+}$ is the primary cause of concentration quenching.

The following equation show how to compute the decay curves [15], [16]:

$$I = A\exp(-t/\tau_R) + B \quad (4)$$

the decay period is t , the relative fluorescence intensity is I , and the fluorescent duration is τ_R . A , along with B , will be constants [15]. $A=7.97\pm 50.20$, $B=-2.67\pm 0.85$, $\tau_R=0.84\pm 0.006$ ms are the fitting results. The inset of Figure 5 shows the relation between the phosphor's fluorescent lifespan and Tb^{3+} . Fluorescence lifespan values fell from 0.85 ms to 0.75 ms when Tb^{3+} content increased from $x=0.01$ to $x=0.15$. The reason for this is that when the amount of Tb^{3+} is low, the distance between Tb^{3+} is relatively large, therefore it is possible to ignore the interactivity among the centers of luminescence. On the other hand, when the amount of Tb^{3+} is higher, resonant power shift formations may exist. And it is possible to exploit these in the form of non-radioactive centers of extra channels so that the exterior can be reached.

Color uniformity is only one of many criteria to consider when assessing WLED color quality. Color quality cannot appraise well with a high color homogeneity index [17]-[19]. As a result, contemporary studies have developed a color rendering index (CRI) as well as a color quality scale (CQS). When illumination shines on the color rendering index, it determines the exact color of an object. The color imbalance happened when the green light is excessive abundance compared to the other three principal colors: blue, yellow, and green. This inequality has an effect on WLED's hue output, causing a penalty in hue fidelity. The findings from Figure 5 exhibit an inappreciable penalty in CRI if the remote phosphor $\text{Gd}_2(\text{WO}_4)_3:\text{Tb}^{3+}$ layer is present. Regardless, as CRI is merely a CQS's flaw, these are tolerable [20]-[22]. When we put CRI and CQS on a scale, CQS would be highly crucial as well as harder to attain. It appears to be an index based on certain aspects, with the first being CRI, the second being observer's preference, with the third being the hue coordinate. With such predominant factors, CQS would be a genuine overall assessment for hue quality [23]-[26]. Figure 6 shows the CQS increase with the remote phosphor $\text{Gd}_2(\text{WO}_4)_3:\text{Tb}^{3+}$ layer being added. In addition, even when the concentration of $\text{Gd}_2(\text{WO}_4)_3:\text{Tb}^{3+}$ rises, CQS considerably does not change unless it exceeds 10% wt. CRI, as well as CQS, notably abbreviate when $\text{Gd}_2(\text{WO}_4)_3:\text{Tb}^{3+}$ concentrations surpass 10% wt. thanks to severe waste of hue caused by green dominance. Before utilizing $\text{Gd}_2(\text{WO}_4)_3:\text{Tb}^{3+}$, proper concentration selection is critical.

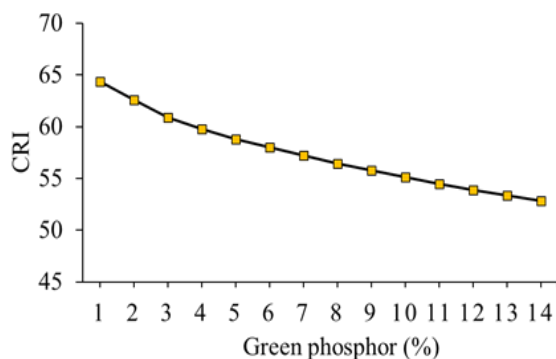


Figure 5. The relation between CRI in the WLED device and $\text{Gd}_2(\text{WO}_4)_3:\text{Tb}^{3+}$ content

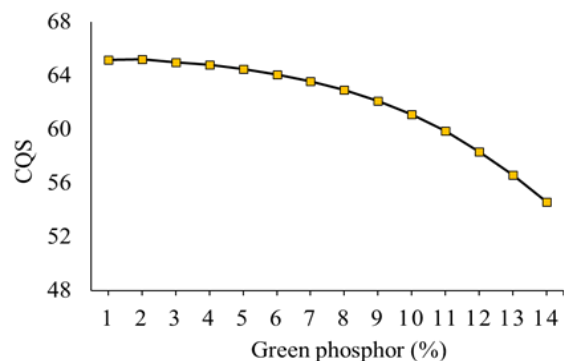


Figure 6. The relation between CQS in the WLED device and $\text{Gd}_2(\text{WO}_4)_3:\text{Tb}^{3+}$ content

4. CONCLUSION

The effect of $Gd_2(WO_4)_3:Tb^{3+}$ green phosphorus on the optical properties of a dual-layer phosphorus arrangement is discussed in this work. The study found that $Gd_2(WO_4)_3:Tb^{3+}$ would be a good choice for improving color uniformity based on Monte Carlo computer recreations in the case of WLED devices under hue temperature below 5600 K as well as ones under color temperature exceeding 8500 K. The outcomes from our study managed to yield greater hue output and luminous flux, a difficult task due to the remote configuration of phosphorus. CRI and CQS, on the other hand, have a tiny drawback. The CRI and CQS fall dramatically when the $Gd_2(WO_4)_3:Tb^{3+}$ concentration is increased excessively. As a result, the right concentration must be chosen based on the manufacturer's aims. The article can provide useful insight into generating higher hue consistency as well as lumen in WLED devices.

ACKNOWLEDGEMENTS

This study was financially supported by Van Lang University, Vietnam.

REFERENCES

- [1] Y. Wang, Y. Zhang, D. Li, A. Zhang, H. Wang, H. Jia, and B. Xu, "Tunable white light emission of an anti-ultraviolet rare-earth polysiloxane phosphors based on near UV chips," *Opt. Express*, vol. 29, no. 6, pp. 8997-9011, Mar. 2021, doi: 10.1364/OE.410154.
- [2] H. Liu, Y. Shi, and T. Wang, "Design of a six-gas NDIR gas sensor using an integrated optical gas chamber," *Opt. Express*, vol. 28, no. 8, pp. 11451-11462, Apr. 2020, doi: 10.1364/OE.388713.
- [3] T. Ya. Orudzhev, S. G. Abdullaeva, and R. B. Dzhbarbarov, "Increasing the extraction efficiency of a light-emitting diode using a pyramid-like phosphor layer," *J. Opt. Technol.*, vol. 86, no. 10, pp. 671-676, Dec. 2019, doi: 10.1364/JOT.86.000671.
- [4] P. Kumar and N. K. Nishchal, "Enhanced exclusive-OR and quick response code-based image encryption through incoherent illumination," *Appl. Opt.*, vol. 58, no. 6, pp. 1408-1412, Feb. 2019, doi: 10.1364/AO.58.001408.
- [5] J. Li, *et al.*, "Investigation of stability and optical performance of quantum-dot-based LEDs with methyl-terminated-PDMS-based liquid-type packaging structure," *Opt. Lett.*, vol. 44, no. 1, pp. 90-93, Dec. 2018, doi: 10.1364/OL.44.000090.
- [6] Y. Li, Y. Tang, Z. Li, X. Ding, L. Rao, and B. Yu, "395 nm GaN-based near-ultraviolet light-emitting diodes on Si substrates with a high wall-plug efficiency of 52.0%@350 mA," *Opt. Express*, vol. 27, no. 5, pp. 7447-7457, Mar. 2019, doi: 10.1364/OE.27.007447.
- [7] M. J. Egan, A. M. Colón, S. M. Angel, and S. K. Sharma, "Suppressing the multiplex disadvantage in photon-noise limited interferometry using cross-dispersed spatial heterodyne spectrometry," *Appl. Spectrosc.*, vol. 75, no. 2, pp. 208-215, Feb. 2021, doi: 10.1177/0003702820946739.
- [8] J. X. Yang, D. Li, L. Gang, E. Y. B. Pun, and L. Hai, "Photon quantification in Ho³⁺/Yb³⁺ co-doped opto-thermal sensitive fluorotellurite glass phosphor," *Appl. Opt.*, vol. 59, no. 19, pp. 5752-5763, May. 2020, doi: 10.1364/AO.396393.
- [9] J. Hao, H. L. Ke, L. Jing, Q. Sun, and R. T. Sun, "Prediction of lifetime by lumen degradation and color shift for LED lamps, in a non-accelerated reliability test over 20,000 h," *Appl. Opt.*, vol. 58, no. 7, pp. 1855-1861, Mar. 2019, doi: 10.1364/AO.58.001855.
- [10] Y. P. Chang, J.-K. Chang, H.-A. Chen, S.-H. Chang, C.-N. Liu, P. Han, and W.-H. Cheng, "An advanced laser headlight module employing highly reliable glass phosphor," *Opt. Express*, vol. 27, no. 3, pp. 1808-1815, Feb. 2019, doi: 10.1364/OE.27.001808.
- [11] Y. Yang, C. Chen, P. Du, X. Deng, J. Luo, W.-D. Zhong, and L. Chen, "Low complexity OFDM VLC system enabled by spatial summing modulation," *Opt. Express*, vol. 27, no. 21, pp. 30788-30795, Oct. 2019, doi: 10.1364/OE.27.030788.
- [12] I. Fujieda, Y. Tsutsumi, and S. Matsuda, "Spectral study on utilizing ambient light with luminescent materials for display applications," *Opt. Express*, vol. 29, no. 5, pp. 6691-6702, Mar. 2021, doi: 10.1364/OE.418869.
- [13] N. C. A. Rashid *et al.*, "Spectrophotometer with enhanced sensitivity for uric acid detection," *Chin. Opt. Lett.*, vol. 17, no. 8, pp. 081701, May. 2019, doi: 10.3788/COL201917.081701.
- [14] A. Adnan, Y. Liu, C. W. Chow, and C. H. Yeh, "Demonstration of non-hermitian symmetry (NHS) serial-complex-valued orthogonal frequency division multiplexing (SCV-OFDM) for white-light visible light communication (VLC)," *OSA Continuum*, vol. 3, no. 5, pp. 1163-1168, Mar. 2020, doi: 10.1364/OSAC.391483.
- [15] G. Xia, Y. Ma, X. Chen, S. Q. Jin, and C. Huang, "Comparison of MAP method with classical methods for bandpass correction of white LED spectra," *J. Opt. Soc. Am. A*, vol. 36, no. 5, pp. 751-758, May. 2019, doi: 10.1364/JOSAA.36.000751.
- [16] S. Kashima, M. Hazumi, H. Imada, N. Katayama, T. Matsumura, Y. Sekimoto, and H. Sugai, "Wide field-of-view crossed Dragone optical system using anamorphic aspherical surfaces," *Appl. Opt.*, vol. 57, no. 15, pp. 4171-4179, 2018, doi: 10.1364/AO.57.004171.
- [17] J. Chen, B. Fritz, G. Liang, X. Ding, U. Lemmer, and G. Gomard, "Microlens arrays with adjustable aspect ratio fabricated by electroforming and their application to correlated color temperature tunable light-emitting diodes," *Opt. Express*, vol. 27, no. 4, pp. A25-A38, Feb. 2019, doi: 10.1364/OE.27.000A25.
- [18] S. Jeon, S. Kim, J. Choi, I. Jang, Y. Song, W. H. Kim, and J. P. Kim, "Optical design of dental light using a remote phosphor light-emitting diode package for improving illumination uniformity," *Appl. Opt.*, vol. 57, no. 21, pp. 5998-6003, Jul. 2018, doi: 10.1364/AO.57.005998.
- [19] T. Hu *et al.*, "Demonstration of color display metasurfaces via immersion lithography on a 12-inch silicon wafer," *Opt. Express*, vol. 26, no. 15, pp. 19548-19554, Jul. 2018, doi: 10.1364/OE.26.019548.
- [20] L. Li, Y. Zhou, F. Qin, Y. Zheng, and Z. Zhang, "On the Er³⁺ NIR photoluminescence at 800 nm," *Opt. Express*, vol. 28, no. 3, pp. 3995-4000, Feb. 2020, doi: 10.1364/OE.386792.
- [21] H. E. A. Mohamed, K. Hkiri, M. Khenfouch, S. Dhlamini, M. Henini, and M. Maaza, "Optical properties of biosynthesized nanoscaled Eu₂O₃ for red luminescence applications," *J. Opt. Soc. Am. A*, vol. 37, no. 11, pp. C73-C79, Aug. 2020, doi: 10.1364/JOSAA.396244.
- [22] A. K. Dubey, M. Gupta, V. Kumar, and D. S. Mehta, "Laser-line-driven phosphor-converted extended white light source with uniform illumination," *Appl. Opt.*, vol. 58, no. 9, pp. 2402-2407, Mar. 2019, doi: 10.1364/AO.58.002402.
- [23] J. Miao *et al.*, "Effect of Yb³⁺ concentration on upconversion luminescence and optical thermometry sensitivity of La₂MoO₆:Yb³⁺, Er³⁺ phosphors," *Appl. Opt.*, vol. 60, no. 6, pp. 1508-1514, Feb. 2021, doi: 10.1364/AO.412313.

- [24] S. S. Panda, H. S. Vyas, and R. S. Hegde, "Robust inverse design of all-dielectric metasurface transmission-mode color filters," *Opt. Mater. Express*, vol. 10, no. 12, pp. 3145-3159, Nov. 2020, doi: 10.1364/OME.409186.
- [25] D. Yan, S. Zhao, H. Wang, and Z. Zang, "Ultrapure and highly efficient green light emitting devices based on ligand-modified CsPbBr₃ quantum dots," *Photon. Res.*, vol. 8, no. 7, pp. 1086-1092, Apr. 2020, doi: 10.1364/PRJ.391703.
- [26] T. W. Kang *et al.*, "Enhancement of the optical properties of CsPbBr₃ perovskite nanocrystals using three different solvents," *Opt. Lett.*, vol. 45, no. 18, pp. 4972-4975, Sep. 2020, doi: 10.1364/OL.401058.

BIOGRAPHIES OF AUTHORS



Dieu An Nguyen Thi    received a master of Electrical Engineering, HCMC University of Technology and Education, VietNam. Currently, she is a lecturer at the Faculty of Electrical Engineering Technology, Industrial University of Ho Chi Minh City, Viet Nam. Her research interests are Theoretical Physics and Mathematical Physics. She can be contacted at email: nguyenthidieuan@iuh.edu.vn.



Nguyen Doan Quoc Anh    was born in Khanh Hoa province, Vietnam. He has been working at the Faculty of Electrical and Electronics Engineering, Ton Duc Thang University. Quoc Anh received his PhD degree from National Kaohsiung University of Science and Technology, Taiwan in 2014. His research interest is optoelectronics. He can be contacted at email: nguyendoanquocanh@tdtu.edu.vn.



Phan Xuan Le    received a Ph.D. in Mechanical and Electrical Engineering from Kunming University of Science and Technology, Kunming city, Yunnan province, China. Currently, He is a lecturer at the Faculty of Engineering, Van Lang University, Ho Chi Minh City, Viet Nam. His research interests are Optoelectronics (LED), Power transmission and Automation equipment. He can be contacted at email: le.px@vlu.edu.vn.